swiss physical society

Nr. 60
Januar 2020

SPG MITTEILUNGEN
COMMUNICATIONS DE LA SSP

AUSZUG - EXTRAIT

Progress in Physics (72)

Ultrathin Layers – Big Effect: Functional Coatings by Plasma Polymerization

Dirk Hegemann, Empa, Swiss Federal Laboratories for Materials Science and Technology, Plasma & Coating Group, Lerchenfeldstrasse 5, 9014 St. Gallen, dirk.hegemann@empa.ch

Progress in Physics (72)

Ultrathin Layers – Big Effect: Functional Coatings by Plasma Polymerization

Dirk Hegemann, Empa, Swiss Federal Laboratories for Materials Science and Technology, Plasma & Coating Group, Lerchenfeldstrasse 5, 9014 St. Gallen, dirk.hegemann@empa.ch

Plasma polymerization defines the process to deposit a so-called "plasma polymer film" (PPF) via activation of a gaseous compound (so-called "monomer") in a low-temperature electrical discharge creating reactive intermediates and film-forming species [1]. These species diffuse to material surfaces yielding film growth at highly non-equilibrium conditions. Functional coatings can thus be applied to a variety of different materials in order to modulate their surface properties. Primary processes in the plasma are activated by electron impact, since mainly the electrons pick up energy from the electric field in collisions with the gaseous particles [2]. The heavy particles thus remain "cold" – defining the low-temperature plasma –, whereas the electrons reach a mean energy of several eV, able to break chemical bonds of the monomer molecule. As a consequence, also compounds that commonly cannot be polymerized, such as for example methane, can be used. The resulting PPFs largely differ from conventional polymers by branching, cross-linking and the lack of repeating units.

Examining the reaction rate in the plasma, i.e. the fragmentation and the resulting deposition rate, the film thickness can be adjusted with high precision at almost atomistic scale. Thus, ultrathin layers, multilayers and nanostructures with vertical gradients can be generated by plasma polymerization.

As another consequence of the mobile electrons, all surfaces in close contact with the plasma get negatively charged with respect to the plasma potential, thus accelerating positive ions towards the surface that gain high energies of tens to hundreds of eV. Accordingly, the highly non-equilibrium, energetic conditions at the surface enables the control over the film density and functionality during film growth – film properties ranging from soft, polymer-like to hard, inorganic coatings are permitted.

Herein, ultrathin plasma polymer layers (with a thickness below about 20 nm) are investigated that serve as an effective barrier to separate a material's surface from the environment, which can be used in different ways to add functionality to the material (Figure 1). As monomers, methane (CH_4) and hexamethyldisiloxane (HMDSO, $(CH_3)_3$–Si–O–Si–$(CH_3)_3$) are discussed in more detail.

The physics behind plasma polymerization

The available energy in the gas discharge, typically represented by the electron energy distribution function (EEDF), allows a plurality of reactions yielding excitation, dissociation and ionization of the monomeric species and their fragments as well as of optionally added carrier and further reactive gases. In-depth understanding and modelling of plasma polymerization processes on a microscopic level thus requires to take account of all involved reaction rates and related cross sections, which are only partially known (Figure 2). For many compounds, however, the film-forming species could be identified due to their high sticking probability, and the corresponding plasma-chemical reaction pathway via dissociation of vibrationally excited states can be predicted.

At typical conditions in a CH_4 plasma with a mean electron energy of 5 eV, for example, approximately hundred times more neutral fragments are observed as ions, since more electrons have energies meeting the threshold energy of ~8 eV for dissociation, whereas ionization starts at ~13 eV with even lower ionization cross sections. Hence, plasma polymerization mainly proceeds via neutral radicals acting as film-forming species.

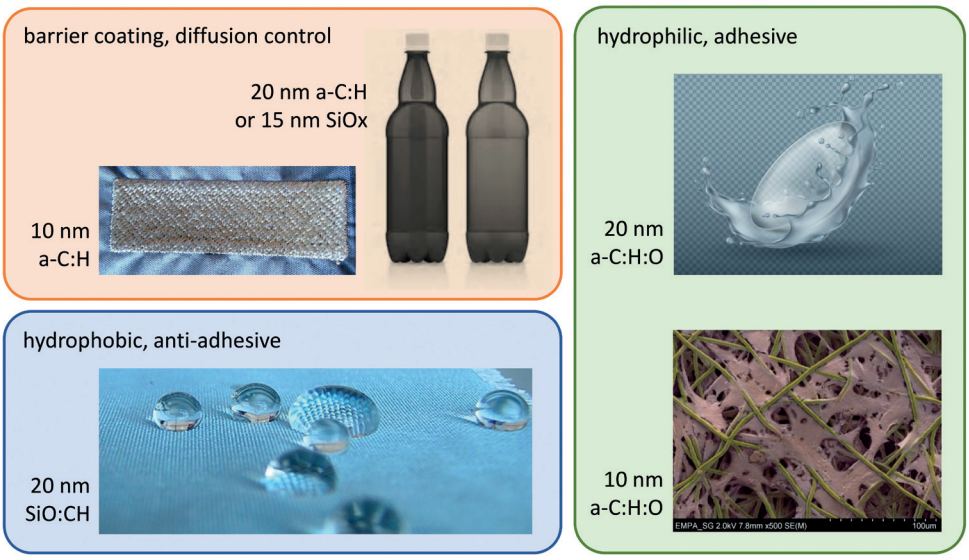

Figure 1. Typical applications for ultrathin plasma polymer films as used for the coating on PET bottles (improving shelf life), textile electrodes (enhancing stability of the electrically conductive Ag-coated yarn), water-repellant fabrics (improving durability and breathability), contact lenses (improving wearing comfort), and tissue engineering (enhancing cell growth on scaffolds).

As a simplified approach, one average reaction rate for the generation of film-forming species might be assumed. Introducing an apparent energy barrier with threshold energy, E_{th}, for activation reactions yielding film-forming species of density, n_{dep}, by electron impact collisions with electron density, n_e, and monomer density, n_m, assuming one averaged collision frequency for activation of the monomer, $\nu_a(E_{th})$, it can simply be noted that

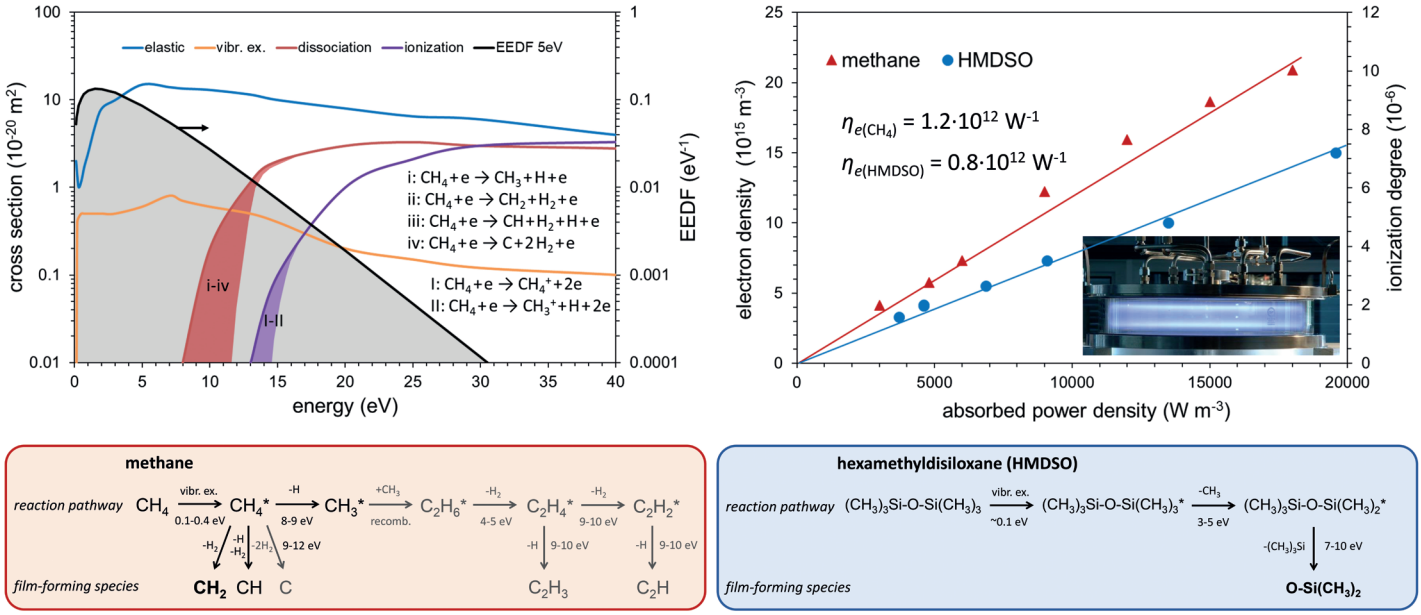

Figure 2. Electron impact reaction cross sections for methane indicating threshold energies for vibrational excitation, dissociation and ionization (left). The grey shaded area gives the electron energy distribution function (EEDF) for a mean electron energy of 5 eV. Electron densities increase linearly with absorbed power density in plasma polymerization processes with a process-depending power coupling coefficient, η_e (right). The inset shows the used capacitively-coupled plasma reactor set-up at a pressure of 10 Pa yielding ionization degrees between 10^{-6} and 10^{-5}. The predicted plasma chemical reaction pathways for methane and HMDSO are added indicating the main film-forming species (below).

$$\frac{dn_{dep}}{dt} = n_e \nu_a \qquad (1)$$

where

$$\nu_a = n_m \langle \sigma_a \cdot v_e \rangle \qquad (2)$$

with the cross section for the overall activation reaction, σ_a, and the electron velocity, v_e [3]. The flux of film-forming species originating from the plasma volume, V_{pl}, towards the deposition area, A_{dep}, can then be given by [2]

$$\Gamma_{dep} = \frac{V_{pl}}{A_{dep}} \frac{dn_{dep}}{dt} = \frac{V_{pl}}{A_{dep}} n_e \nu_a \qquad (3)$$

For polymerizing plasmas with one type of monomer, n_e is typically found to be linear with the absorbed power density, W_{abs} / V_{pl}, in the plasma (see Figure 2):

$$n_e = \eta_e \frac{W_{abs}}{V_{pl}} \qquad (4)$$

introducing the power coupling coefficient, η_e (in [W^{-1}]), that connects microscopic and macroscopic quantities. From Equation (3) and dividing both sides by the monomer gas flow rate, F_m, and normalizing to standard temperature, T_0, and standard pressure, p_0, (k: Boltzmann constant) the (dimensionless) degree of conversion of monomer into film-forming species is given by:

$$c = \frac{kT_0}{p_0} \frac{A_{dep}}{F_m} \Gamma_{dep} = \frac{kT_0}{p_0} \frac{W_{abs}}{F_m} \eta_e \nu_a \qquad (5)$$

The right hand side now contains the well-known reaction parameter, power input per monomer gas flow rate, W/F_m (in [J m^{-3}]), as frequently used for plasma polymerization, which is equivalent to the specific energy input (*SEI*), i.e. the average energy available per monomer molecule in the plasma, E_{pl}, (in [eV]; eE_{pl} in [J] – e: electron charge):

$$SEI = E_{pl} = \frac{kT_0}{ep_0} \frac{W_{abs}}{F_m} \qquad (6)$$

While Γ_{dep} is difficult to assess directly, it is proportional to the mass deposition rate for constant sticking probability, s, and constant molecular mass of the deposited species, M_{dep}, (N_A: Avogadro number):

$$R_m = s \frac{M_{dep}}{N_A} \Gamma_{dep} \qquad (7)$$

Hence, the straightforward evaluation of deposition rates can give important insights into plasma polymerization processes, and the conversion depending on R_m and E_{pl} can be given by combining Equation (5) and (7):

$$c = \frac{kT_0}{p_0} \frac{A_{dep}}{F_m} \frac{N_A}{s\, M_{dep}} R_m = eE_{pl} \eta_e \nu_a \qquad (8)$$

While film-forming species are mainly uncharged highly reactive radicals, the growing film is constantly bombarded by ions such as e.g. CH_4^+ and CH_3^+ in methane or HMDSO plasmas yielding formation of radical sites and densification at highly non-equilibrium conditions [4]. The deposited energy can be obtained from ion flux, Γ_i, and ion energy, E_i, incident on the surface with respect to the deposition rate:

$$E_d = E_i \frac{\Gamma_i}{s\, \Gamma_{dep}} \qquad (9)$$

Film properties such as film density, porosity and functional group density can thus be controlled by adjusting E_d. A minimum energy around 10 eV per condensing molecule is required to create radical sites and covalent bonding to support the formation of highly stable plasma polymer films. Higher energies limit the incorporation of (terminal) functional groups such as $–CH_3$, –COOH, –C-OH etc. due to enhanced crosslinking showing increasing hardness of the PPFs up to ~50 eV per molecule [5]. Even higher deposited energies can result in strong etching conditions.

Plasma polymerization of methane and HMDSO

Commonly used monomers for plasma polymerization comprise CH_4 and HMDSO to deposit amorphous hydrocarbon coatings, a-C:H, and silicone-like coatings, SiO:CH, respectively. To investigate the plasma polymerization processes in depth, a capacitively-coupled plasma reactor has been used that enables a confined uniform plasma volume and well-defined deposition conditions (see Figure 2). The observed deposition rates reveal a linear increase with the average energy per monomer molecule, E_{pl}, up to the threshold energy, E_{th}, which represents the apparent activation energy for the considered plasma polymerization process (Figure 3). Hence, the averaged collision frequency for activation of the monomer, $\nu_a(E_{th})$, appears to be constant for $E_{pl} \leq E_{th}$, according to Equation (8). For $E_{pl} > E_{th}$, the deposition rate starts to saturate revealing an Arrhenius-like behavior depending on E_{pl} instead of temperature, kT, from which E_{th} can be deduced. The corresponding Arrhenius-like fit gives apparent activation energies of ~10 eV for CH_4 and ~13 eV for HMDSO, which is in excellent agreement with the predicted overall reaction pathway to generate film-forming species (see Figure 2 and 3). The process conditions can thus be adjusted to allow sufficient fragmentation in the gas phase, while controlling deposition rates by F_m and E_{pl}.

The used reactor set-up and pressure (10 Pa) yields a maximum conversion of monomer into film-forming species of 30 - 40 % assuming a sticking probability around one at sufficient energy provided for film growth. The conversion could be further enhanced by raising the power coupling coefficient, e.g. by reducing pressure, adding carrier gases (Ar) or using different plasma sources such as inductively-coupled and microwave plasmas.

Considering surface conditions with moderate E_d around 10 - 20 eV, polymer-like a-C:H and SiO:CH films are formed, whereby the film density increases with E_d from about 1.1 to 1.5 g cm^{-3} [6]. In this way, the permeability and hydrophobicity of such PPFs can be controlled for barrier coatings and water-repellency on soft, polymeric substrates such as PET bottles or textiles [6-8]. In order to observe continuous closed films, a thickness of around 10 - 20 nm is required allowing fast processing with coating times as low as 2 s [7].

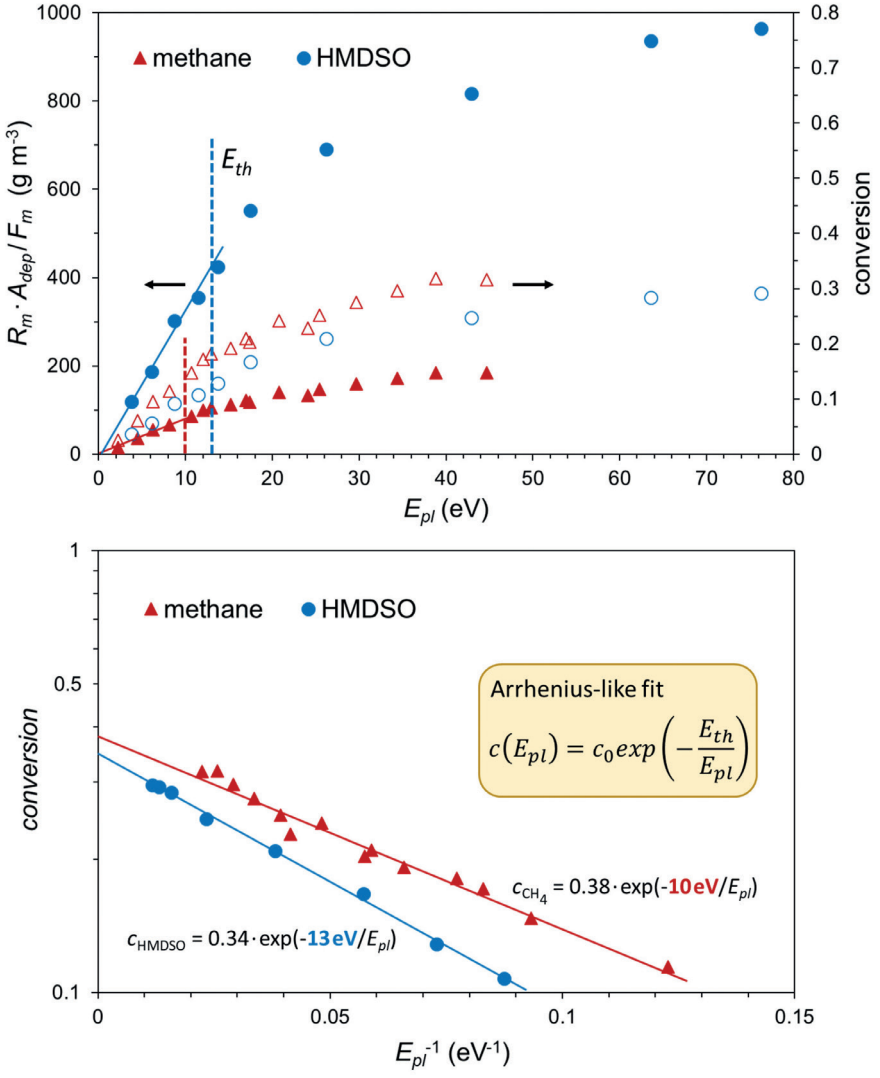

Figure 3. Normalized deposition rates for CH_4 and HMDSO plasmas showing a linear increase with the energy invested per monomer particle, E_{pl}, up to a threshold energy, E_{th} (top). While the absolute deposition rates are higher in HMDSO due to larger film-forming species, the conversion, i.e. the percentage of monomer molecules incorporated into film growth, is comparable (open symbols). The conversion at higher energies reveals an Arrhenius-like behavior, where temperature, kT, is replaced by E_{pl} (bottom). The apparent threshold energies for plasma polymerization can thus be deduced yielding ~10 eV for CH_4 and ~13 eV for HMDSO.

Besides the control of energy input, film properties can strongly be influenced by gas composition, e.g. by addition of oxygen in the plasma. Gas ratios of O_2 / CH_4 ≤ 1 result in highly functional nanolayers of a-C:H:O PPFs that, for example, increase the wearing comfort for contact lenses manufactured at low costs in a dry and environmentally friendly process [9]. Likewise, the wettability and adhesion properties can be enhanced, e.g. for biomedical applications [10, 11]. Oxidation of HMDSO, on the other hand, requires higher O_2 / HMDSO ratios in order to oxidize the hydrocarbon side groups as well as the side products, the SiC_3H_9 radicals, ideally yielding two SiO_2 film-forming units per HMDSO molecule [12]. High oxidation and densification yields ultrathin SiO_2-like PPFs that are used as barrier coatings on PET bottles and further packaging materials.

Very recent activities concern the initial adsorption of proteins as well as bacterial adhesion on surfaces, where the deposition of a 2 nm thick SiO:CH coating from a HMDSO plasma serves as a cover layer separating the substrate material from the biological medium. For the protein experiments with bovine serum albumin (BSA), the cover layer was deposited on a nanoporous SiO_x base layer, i.e. less densified as a barrier coating, thus providing a hydrophilic subsurface structure. Interestingly, it was observed that the protein adsorption is affected by water intrusion through the cover layer depending on the free volume, i.e. the porosity, of the subsurface [13]. Formation

of fixed dipoles due to trapped water molecules might induce an additional long-range interaction that can be exploited to control initial protein adsorption independent of surface properties. For the bacterial adhesion with *E. coli*, the 2 nm SiO:CH cover layer was deposited on silicone elastomers showing varying stiffness by modifying the PDMS:crosslinker ratio. It has been controversially discussed whether the viscoelastic properties of a material influence bacterial adhesion yielding stronger adhesion on softer material. The ultrathin plasma layer maintained the viscoelastic properties by equalizing the surface properties. As an important finding, bacterial adhesion was found to hardly depend on viscoelastic properties but on the stickiness of the surface [14].

Conclusion

Plasma polymerization, i.e. the generation of film-forming species in a low-temperature plasma, can be controlled by gas composition as well as the energy available per monomer molecule in the gas phase and during film growth at the surface. Thus, ultrathin coatings can be deposited with high precision on a variety of substrate materials enabling functional surfaces with tailored properties by fast, economic and sustainable processes.

References

[1] H. Biederman, *Plasma Polymer Films*, Imperial College Press, London, UK 2004.
[2] J. Reece Roth, *Industrial Plasma Engineering*, Inst. Phys. Publ., Bristol, USA 2001.
[3] D. Hegemann, *J. Phys. D: Appl. Phys.* **46**, 205204 (2013).
[4] D. Hegemann, B. Hanselmann, N. Blanchard, M. Amberg, *Contr. Plasma Phys.* **54**, 162–169 (2014).
[5] S. Peter, K. Graupner, D. Grambole, F. Richter, *J. Appl. Phys.* **102**, 053304 (2007).
[6] D. Hegemann, Plasma Polymer Deposition and Coatings on Polymers. In: *Comprehensive Materials Processing*, Vol. 4, Ed. D. Cameron, Elsevier Ltd., 2014, pp 201–228.
[7] A. Shirakura, Ma. Nakaya, Y. Koga, H. Kodama, T. Hasebe, T. Suzuki, *Thin Solid Films* **494**, 84 (2006).
[8] M. Amberg, M. Vandenbossche, D. Hegemann, *Surf. Coat. Technol* **336**, 29 (2018).
[9] H. Yasuda, Y. Matsuzawa, *Plasma Process. Polym.* **2**, 507 (2005).
[10] F. Awaja, S. Zhang, N. James, D. R. McKenzie, *Plasma Process. Polym.* **7**, 1010 (2010).
[11] A. G. Guex, F. M. Kocher, G. Fortunato, E. Körner, D. Hegemann, T. P. Carrel, H. T. Tevaearai, M. N. Giraud, *Acta Biomater.* **8**, 1481 (2012).
[12] M. Deilmann, H. Halfmann, S. Steves, N. Bibinov, P. Awakowicz, *Plasma Process. Polym.* **6**, S695 (2009).
[13] E. Bülbül, P. Rupper, T. Geue, L. Bernard, M. Heuberger, D. Hegemann, *ACS Appl. Mater. Interfaces* **11**, 42760 (2019).
[14] F. Pan, S. Altenried, M. Liu, D. Hegemann, E. Bülbül, J. Moeller, W. W. Schmahl, K. Maniura-Weber, Q. Ren, *Mater. Horiz.* DOI: 10.1039/C9MH01191A (2019).